

Purdue University Purdue e-Pubs

International Refrigeration and Air Conditioning
Conference

School of Mechanical Engineering

2018

Numerical Investigation on Effects of Sub-cooling Methods on Performance of Multi-split Variable Refrigerant Flow Systems with Bypass and Vapor Injection Techniques

Byung-chae Min
bcmim@pusan.ac.kr

Sang-kyung Na
Graduate School of Mechanical Engineering, Pusan National University, Busan, Republic of (South Korea),
naskng@pusan.ac.kr

Hyeongjun Kim
Pusan National University, Korea, Republic of (South Korea), kimhyeongjun@pusan.ac.kr

G.M. Choi
Pusan National University, choigm@pusan.ac.kr

Follow this and additional works at: <https://docs.lib.purdue.edu/iracc>

Min, Byung-chae; Na, Sang-kyung; Kim, Hyeongjun; and Choi, G.M., "Numerical Investigation on Effects of Sub-cooling Methods on Performance of Multi-split Variable Refrigerant Flow Systems with Bypass and Vapor Injection Techniques" (2018). *International Refrigeration and Air Conditioning Conference*. Paper 1948.
<https://docs.lib.purdue.edu/iracc/1948>

This document has been made available through Purdue e-Pubs, a service of the Purdue University Libraries. Please contact epubs@purdue.edu for additional information.

Complete proceedings may be acquired in print and on CD-ROM directly from the Ray W. Herrick Laboratories at <https://engineering.purdue.edu/Herrick/Events/orderlit.html>

Numerical investigation on effects of sub-cooling methods on performance of multi-split variable refrigerant flow systems with bypass and vapor injection cycles

Byungchae Min¹, Sangkyung Na¹, Hyungjun Kim¹, Gyungmin Choi^{2*}

¹Graduated School of Mechanical Engineering, Pusan National University,
Busan, Korea

(bcmin@pusan.ac.kr, naskng@pusan.ac.kr, kimhyungjun@pusan.ac.kr)

²Department of Mechanical Engineering, Pusan National University,
Busan, Korea

(choigm@pusan.ac.kr)

ABSTRACT

The pipeline connected between outdoor units and indoor units is lengthened in the VRF systems because the VRF systems are generally used in light commercial buildings. Therefore, a sub-cooler is installed in the VRF systems to avoid flash gas caused by pressure drop and heat transfer in the liquid pipeline. Usually, the liquid refrigerant in the pipeline can be cooled by bypass and refrigerant injection techniques with an internal heat exchanger (IHX) and electric expansion valve (EEV). In this study, the performance of the VRF systems using bypass and refrigerant injection cycles are compared by numerical method. The simulation for multi-split VRF is developed with considering application of vapor injection and bypass cycle and validated with experimental data. The bypass and refrigerant injection have improvement potential for cooling capacity by 3.11% and 15.5%, respectively due to increasing enthalpy difference in evaporators. The vapor injection technique has more improvement potential of performance than bypass technique. Subcooling degree at inlet of EEV is above 10°C degree in two systems, which can avoid flash gas generation.

Keywords : Multi-split VRF system, Bypass cycle, Refrigerant injection, Subcooling, Flash gas

1. INTRODUCTION

A multi-split variable refrigerant flow (VRF) system has been used recently in commercial and residential buildings as cooling and heating units under hot climates and cold climates because of its high part-load efficiency, individual control in separated zones, and saving installing space. The multi-split VRF system consists generally of one or several outdoor units and several indoor units in small and middle size buildings. Usually, the outdoor unit is installed at the top or ground out of the building, hence, gas and liquid pipeline between the outdoor units and indoor units could be lengthened by about 150m. (Afify, 2008) The pressure drop and heat transfer in these pipelines occur, thereby generating flash gas at inlet of EEV in indoor units, and inducing high suction temperature at compressor suction port. The flash gas at inlet of EEV leads to noise near the EEV and degrading performance of the system, and the heat transfer in the gas pipeline increases the suction temperature thereby decreasing volumetric efficiency of a compressor.

The bypass cycle and refrigerant injection cycle have been applied to the heat pump system in order to enhance performance of the system, prevent the flash gas generation, and avoid high discharge temperature in a compressor under severe weather conditions. In these two cycles, the refrigerant from the condenser is separated into two paths in the internal heat exchanger (IHX). Then a portion of the refrigerant is expanded through the subcooler electronic expansion valve (SC EEV), and the remainder flows in main pipeline in order to increase subcooling degree at liquid pipeline by heat exchange inside the IHX. The heated refrigerant from the IHX is injected to the accumulator in the suction line or a compression chamber in the compressor. The former is known as a bypass cycle, and the latter is known as refrigerant injection cycle. The injected refrigerant could decrease superheating degree at suction port by mixing with the refrigerant from the evaporator in the accumulator, and decreases discharge temperature by low suction temperature for the bypass cycle and intercooling during compression process for the refrigerant injection cycle. Figure 1 shows the schematic diagram of the bypass cycle and refrigerant injection cycle.

Kwon et al (2012) conducted the field performance test for the multi-split VRF system with a subcooler (same as the IHX) and the bypass type cycle. They concluded from the experimental results that the multi-split VRF system with the subcooler has a better performance than the conventional system without the subcooler. Li et al

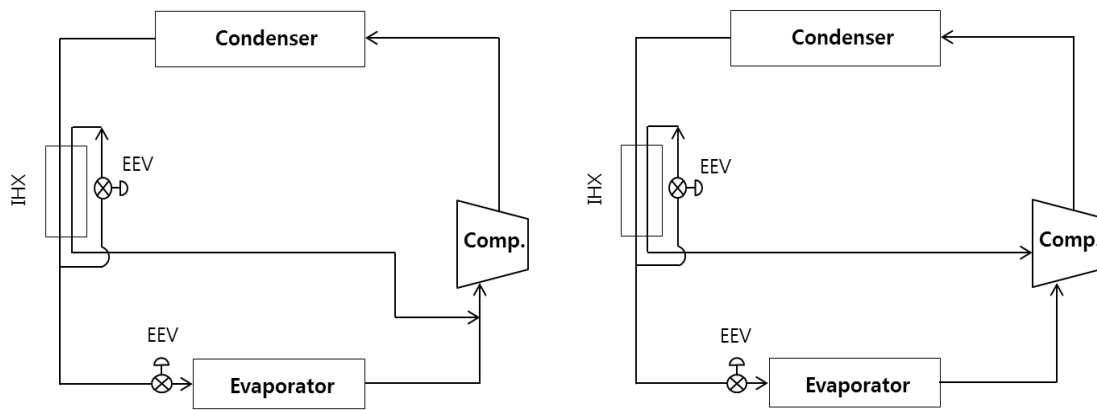


Figure 1 : schematic diagram of bypass and refrigerant injection cycles

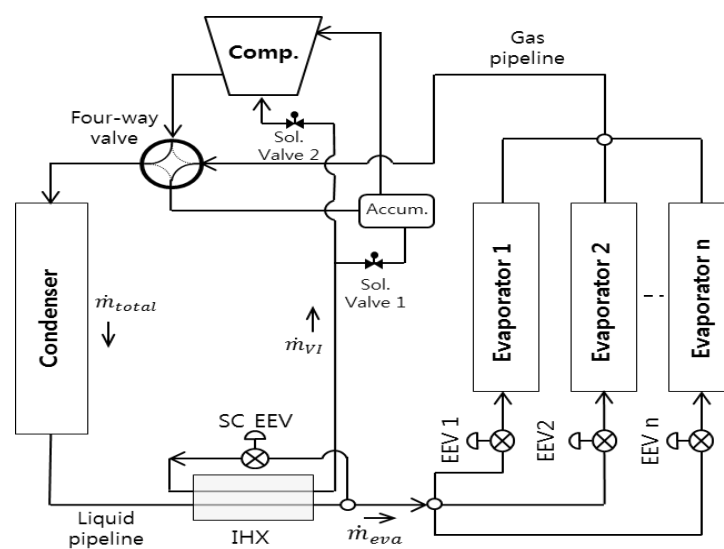


Figure 2 : Schematic diagram of the multi-split VRF system

(2016) carried out the simulation study on effects of three factors such as the length of the main pipeline, the capacity of the IHX (called as subcooler heat exchanger in this paper), and the bypass refrigerant mass flow rate ratio for the bypass cycle of the multi-split VRF system. In this study, it was observed that the subcooler has little benefit on the cooling capacity and COP of a multi-split VRF system. Cho et al. (2016) compared performance between R410A and R32 multi-split VRF system with vapor-injection cycle. In this study, performance of the systems with R410A and R32 in both cooling and heating modes was enhanced by the vapor injection in the scroll compressor.

As stated previously, application of both bypass and refrigerant injection cycles is expected to improve the performance of the multi-split VRF system and prevent flash gas generation at inlet of EEVs. These two types could be applied to the same multi-split VRF system by solenoid valves to switch the injection path into the accumulator or the compression chamber. The aim of this study is to compare performance of both systems with variation in bypass and injection refrigerant ratio.

2. DESCRIPTION OF A MULTI-SPLIT VRF SYSTEM

The multi-split VRF system composed of one outdoor unit with rated capacity of 22.4kW and nine indoor units with cooling capacity of 2.5kW was used for the comparison study with bypass and refrigerant injection cycle. Figure 2 shows the schematic diagram of the multi-split VRF system. A heat exchanger in outdoor unit is a condenser, and that in indoor unit is an evaporator under cooling mode, and vice versa under heating mode. Internal heat exchanger (IHX) is used for heat exchange between main liquid line and bypass or injection line to cool the liquid refrigerant in main pipeline. Operating modes for bypass and refrigerant injection cycle can be switched by solenoid valve 1 and 2 in figure 2. On the bypass cycle mode, solenoid valve 1 is opened, and solenoid valve 2 is closed, and on the vapor-injection cycle mode, vice versa. The bypass and injection mass flow rate is adjusted by SC EEV. Table 1 shows the specifications of components used in this study.

Table 1 : Specifications of the major components

Components	Type	Specifications
Compressor	Refrigerant injection scroll compressor	Displacement volume : 48.0 cm ³ /rev Rotational speed : Max. 120Hz
Outdoor unit heat exchanger	Louver fin-tube type (Air to refrigerant)	W1.75 m × H1.21 m × D0.3 m
Indoor unit heat exchanger	Louver fin-tube type (Air to refrigerant)	W1.23 m × H0.241 m × D0.39 m
Subcooler (internal heat exchanger)	Concentric counter flow type (Refrigerant to refrigerant)	-

3. MODELING OF A MULTI-SPLIT VRF SYSTEM

3.1 Scroll compressor

A scroll compressor was modeled with geometry-based thermodynamic approach proposed by Kwon et al. (2017) in order to predict discharge mass flow rate and input power of a scroll compressor for the bypass and refrigerant injection cycles. The injection process in a scroll compressor depends on diameter of the injection hole, intermediate pressure, evaporating and condenser pressures, and so on. In addition, suction superheating degree also affects suction process and volumetric efficiency for a scroll compressor. Therefore, the geometry-based thermodynamic approach has to be applied to consider these factors. The volumes in a scroll compressor were calculated based on the mathematical model by Chen et al. (2002). The suction, compression, and discharge processes were simulated by thermodynamic models to satisfy mass and energy conservation in the scroll compressor. However, leakages and heat transfer in the compressor were neglected to reduce the calculation time. The experimental data was used for prediction of the performance of a scroll compressor such as motor efficiency and mechanical efficiency data.

The governing equations for mass, temperature, and pressure were expressed in Eqs (1)-(3), respectively.

$$\frac{dm}{d\theta} = \frac{dm_{in}}{d\theta} - \frac{dm_{out}}{d\theta} + \frac{dm_{inj}}{d\theta} \quad (1)$$

$$\frac{dT}{d\theta} = \frac{\left[\frac{dm_i}{d\theta}(h_{in}-h) - \frac{dm_{out}}{d\theta}(h_{out}-h) + \frac{dm_{inj}}{d\theta}(h_{inj}-h) \right] - \left(\frac{dv}{d\theta} - v \frac{dm}{d\theta} \right) \left[\left(\frac{\partial h}{\partial v} \right)_T - v \left(\frac{\partial P}{\partial v} \right)_T \right]}{m \left[\left(\frac{\partial h}{\partial T} \right)_v - v \left(\frac{\partial h}{\partial T} \right)_v \right]} \quad (2)$$

$$\frac{dP}{d\theta} = \left(\frac{\partial p}{\partial T} \right)_v \frac{dT}{d\theta} + \left(\frac{\partial p}{\partial v} \right)_T \frac{dv}{d\theta} \quad (3)$$

The mass flow rates for suction, injection, and discharge process were calculated by Eqs. (4)-(6)

$$\dot{m} = CA \sqrt{\frac{2k}{(k-1)} P_u \rho_u \left\{ P_r^{2/k} - P_r^{(k+1)/k} \right\}} \quad (4)$$

$$P_{cr} = \left(\frac{2}{k+1} \right)^{\frac{k}{k-1}} \quad (5)$$

if $P_r < P_{cr}$, $P_r = \frac{P_{down}}{P_{up}}$

$$\dot{m} = CA \sqrt{\frac{2k}{(k-1)} P_u \rho_u \left\{ \left(\frac{2}{k+1} \right)^{\frac{2}{k-1}} \right\}} \quad (6)$$

Two phase injection in a compression chamber during injection process in the scroll compressor has to be predicted when the two phase injection occurs. The mass flow rate of two phase injection was calculated with an assumption of a homogeneous flow that regards a gas-liquid two phase flow as a single phase flow with apparent physical properties, as Eq. (7) (JSRA, 2018). For the homogeneous model, slip ratio(S) is assumed

Table 2 : Correlations for heat transfer and pressure drop

Heat transfer coefficients	Refrigerant side - Single phase : Gnielinski - Two phase : Condensation : Shah Evaporation : Jung-Radermacher Air side - Forced convection : Wang et al - Natural convection : Churchill and Chu
Pressure drop coefficients	Refrigerant side - Single phase : Churchill - Two phase : Condensation : Lockhart-Martinelli Evaporation : Grönerud

with $S=1$, therefore, two-phase specific volume is :

$$v_{tp} = v_l + x(v_g - v_l) \quad (7)$$

The input power of the compressor was calculated from the results of temperature and pressure calculation from suction to discharge processes. The indicated work was obtained as Eq. (8)

$$W_{ind} = \oint P dV \quad (8)$$

The input power consumed by the scroll compressor was finally obtained with motor and mechanical efficiency data from the experiments, as Eq. (9)

$$W_{comp} = \eta_{motor}\eta_{mech}W_{ind} \quad (9)$$

The bypass ratio and injection ratio are defined as the ratio of the bypass mass flow rate to the total mass flow rate, and the ratio of the injection mass flow rate to the total mass flow rate, respectively.

$$R_{byp} = \frac{\dot{m}_{byp}}{\dot{m}_{total}} \quad \text{and} \quad R_{inj} = \frac{\dot{m}_{inj}}{\dot{m}_{total}} \quad (10)$$

3.2 Heat exchangers (condenser, evaporator, and IHX)

Many heat exchangers are used in the multi-split VRF system as the condensers, evaporators, and an internal heat exchanger. The louver-type fin-tube heat exchangers with counter flow were adopted in outdoor units and indoor units. In this study, these heat exchangers were modeled by the tube-by-tube method and effectiveness-NTU method. For the tube-by-tube method, a particular tube of the heat exchanger is divided as a control volume. The heat transfer in each tube between the refrigerant and air is simulated with average properties at inlet and outlet of each tube with consideration of energy and mass conservation. In the heat exchanger models, there were some assumptions as following:

- The refrigerant flow in the tube is one-dimensional
- Thermal properties of the refrigerant and the air are homogeneous in any cross section
- The refrigerant liquid and vapor phases are in thermodynamic equilibrium
- Air velocity and air temperature in cross section are constant
- The air flow is not mixed between columns
- The gravity of the working fluid is ignored

Correlations of heat transfer and pressure drop for the refrigerant side and air side are summarized in Table 2. In evaporators, dehumidification was simulated with an assumption of the linearization of the condensing process under wet condition as the model proposed by Ragazzi (1995).

3.3 Electronic expansion valve (EEV)

The mass flow rate through the EEVs is predicted by an simple orifice equation :

$$\dot{m}_{main\ EEV} = C_v A \sqrt{\rho_{EEV,i} \Delta P_{EEV}} \quad (11)$$

The inlet condition of the EEVs was determined from the results of IHX calculation, and the outlet condition was determined with assuming the expansion process to be isentropic.

3.4 Pressure drop and heat transfer in pipelines

The heat transfer in pipelines was calculated with natural convection heat transfer correlation for the air side and single or two-phase flow heat transfer correlations in the refrigerant side. The pipelines were insulated by closed cell elastomeric thermal insulation material of 9mm thickness. The heat transfer correlations are summarized in Table 1. The pressure drop inside the pipelines was calculated with considering whether single or two-phase flow. In the single-phase flow region, the pressure drop was evaluated with Churchill correlation (1977) as Eqs. (12)-(14).

$$-\frac{dP}{dL} = f \frac{L}{D} \frac{\rho V^2}{2} \quad (12)$$

$$f = 8 \left[\left(\frac{8}{Re} \right)^{12} + \frac{1}{(A+B)^{1.5}} \right]^{1/12} \quad (13)$$

$$A = \left[2.457 \ln \left(\frac{1}{\left(\frac{7}{Re} \right)^{0.9} + 0.27 \varepsilon/D} \right) \right]^{16} \quad \text{and} \quad B = \left(\frac{37530}{Re} \right)^{16} \quad (14)$$

In two-phase flow region, the pressure drop was evaluated by Grönnerud's correlation (Grönnerud, 1979) as Eqs. (15)-(16).

$$-\frac{dP}{dL} = f_l \frac{L}{D} \frac{\rho_l V^2}{2} \phi_l^2 \quad (15)$$

$$\phi_l^2 = f_{Fr} \left[x + 4(x^{1.8} - x^{10} f_{Fr}^{0.5}) \left[\frac{(\rho_f/\rho_v)}{(\mu_f/\mu_v)^{0.25}} - 1 \right] \right] \quad (16)$$

3.5 Simulation model of the multi-split VRF system

Figure 3 shows the flow chart of simulation for the multi-split VRF system under cooling mode. The component models for the entire system are linked and solved sequentially with the basic rule of mass, energy, and momentum conservation in the multi-split VRF system. The mass flow rate flowing into individual evaporator could be modulated by the EEV opening area according to preset superheating degree at outlet of the evaporator in the real VRF systems. This control method was applied to the simulation in this study.

In the simulation process, the iterative calculation was conducted to satisfy the set values until the relative errors and absolute errors are less than their acceptable values. The relative error and absolute errors are defined as Eqs (17)-(20).

$$e_{sub,cond} = |\Delta T_{sc} - \Delta T_{sc,set}| \leq 0.1 \text{ } ^\circ\text{C} \quad (17)$$

$$e_{sup,eva} = |\Delta T_{sh,e} - \Delta T_{sh,set}| \leq 0.1 \text{ } ^\circ\text{C} \quad (18)$$

$$e_{sup,IHX} = |\Delta T_{sh,inj} - \Delta T_{sh,inj,set}| \leq 0.1 \text{ } ^\circ\text{C} \quad (19)$$

$$e_m = \frac{|\dot{m}_{eva} - \dot{m}_{EEV}|}{\dot{m}_{eva}} \leq 0.1 \text{ } \% \quad (20)$$

$$\dot{m}_{eva} = \dot{m}_{comp} - \dot{m}_{inj} \quad (21)$$

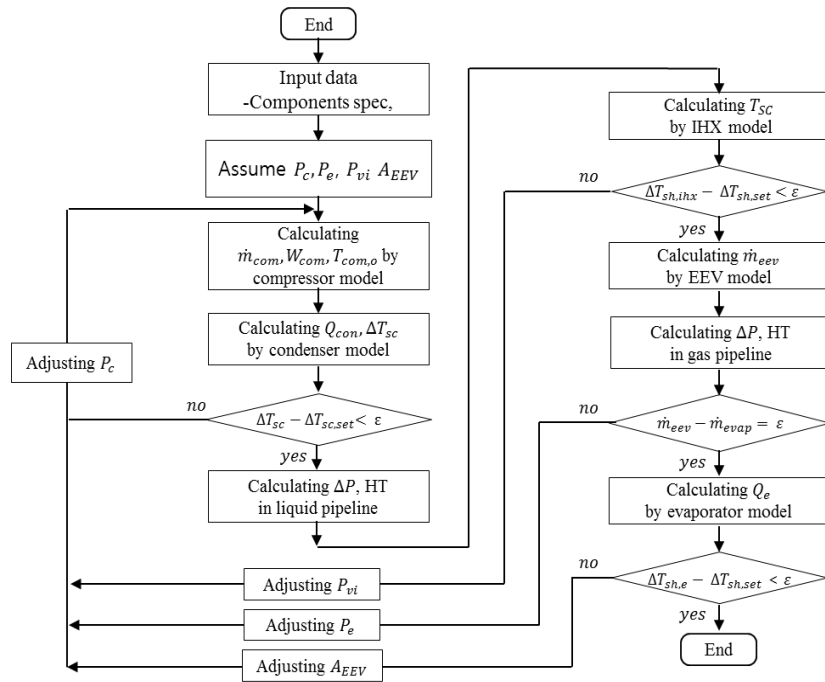


Figure 3 : Flow chart for simulation of the multi-split VRF system

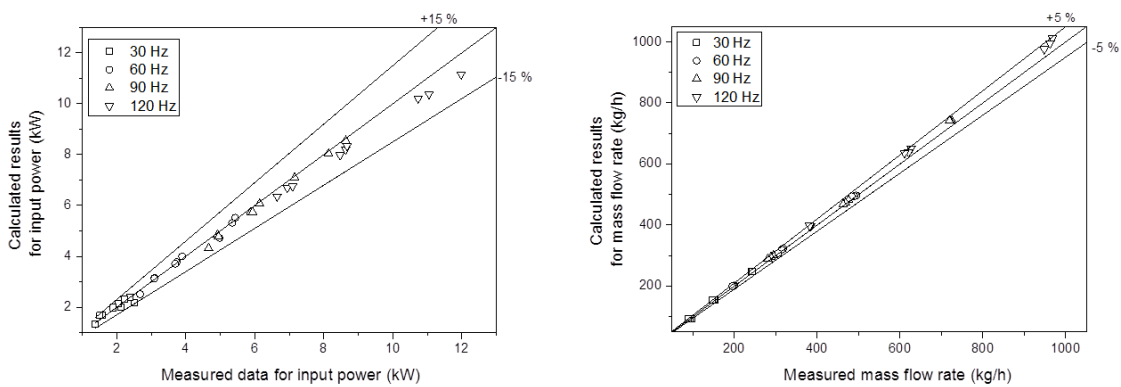


Figure 4 : Validation result of simulation on scroll compressor without refrigerant injection

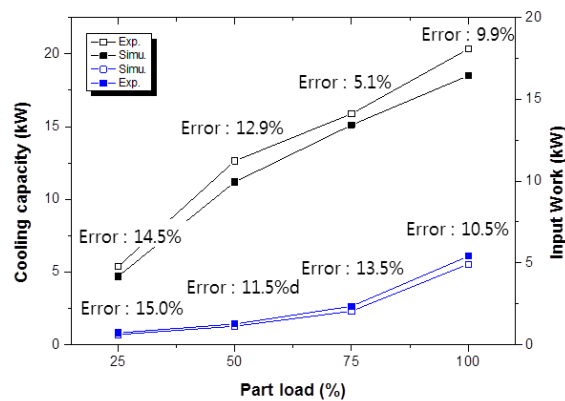


Figure 5 : Validation result of simulation on the multi-split VRF system

4. VALIDATION

In order to verify reliability of a compressor simulation module, simulation results of input power and mass flow rate of a scroll compressor without vapor-injection and bypass cycle are compared to the experimental data

which are obtained from the calorimeter test of a compressor according to the ISO 917. Figure 4 shows the validation results for the scroll compressor without vapor-injection. The calculated results of input power and mass flow rate of a scroll compressor are consistent within 10% and 5%, respectively.

The experimental data for performance of the multi-split VRF system were obtained according to AHRI Standard 1230 to verify the simulation accuracy for the multi-split VRF system. Figure 5 shows the comparison result of the simulation with experimental data with variation in part-load of the system. The simulation result for the multi-split VRF system shows the good agreement within 15%.

5. RESULTS AND DISCUSSION

The comparison simulation on effects of bypass and injection ratio was performed with 100m length of pipelines in the multi-split VRF system under outdoor temperature of 35.0 and 46.1 °C. The bypass ratio varied with change of the ratio as input data in the simulation, and the injection ratio was controlled with variation in intermediate pressure.

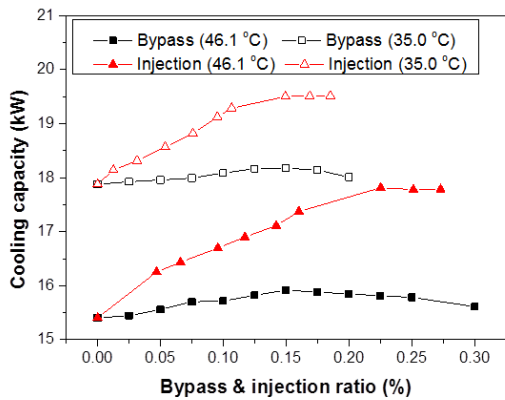


Figure 6 : Cooling capacity

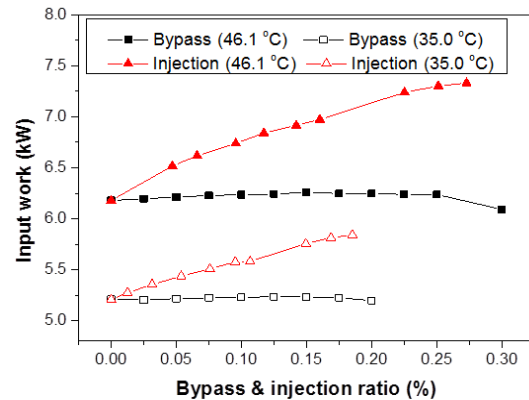


Figure 7 : Input power

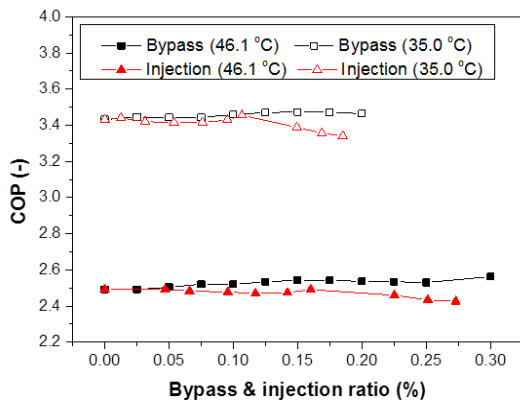


Figure 8 : Coefficient of performance

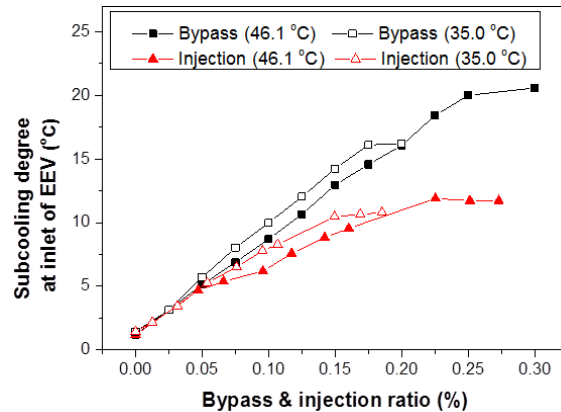


Figure 9 : Subcooling degree

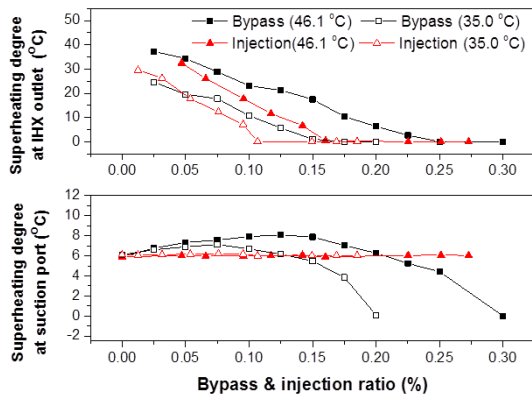


Figure 10 : Superheating degree

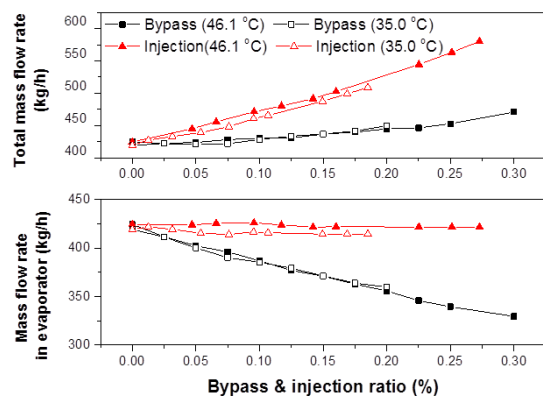


Figure 11 : Mass flow rate

The performance variation of the multi-split VRF system is shown in figure 6 through figure 8 with change in bypass and injection ratio under two outdoor temperature conditions. Cooling capacity and input power of the system with refrigerant injection are higher than those with bypass cycle. However, coefficient of performance of the system with refrigerant injection is lower than that with bypass cycle. Cooling capacity of both systems increases with an increase of the bypass and injection ratio because enthalpy difference in evaporators becomes larger due to an increase of subcooling degree at inlet of EEV as shown in figure 9. The subcooling degree at inlet of EEV increases as the bypass and injection ratio increases due to performance enhancement of heat exchange in IHX. In the IHX, heat exchange occurs between bypass or injection refrigerant with two-phase state and main stream line with sing phase state. Hence, the refrigerant state in the bypass and injection line affects significantly the heat exchange. The smaller superheating degree at outlet of IHX is, the wider the heat transfer area with two-phase state in the bypass and injection line is, which enhances overall heat transfer coefficient in the IHX. Therefore, in figure 9, subcooling degree at inlet of EEV increases with an increase of bypass and injection ratio. As shown in figure 10, superheating degree at outlet of IHX decreases with an increase of bypass and injection ratio, but it reaches 0 degree from specific points. From these points, the heat transfer in IHX occurs as two-phase state in the entire region of the bypass and injection line, and the overall heat transfer coefficient of IHX remains nearly constant. Therefore, subcooling degree at inlet of EEV dese not change in Figure 9. On the bypass mode, cooling capacity increases slightly with an increase of the bypass ratio, but it decreases as the bypass ratio increases more because the mass flow rate in evaporators decrease despite of the increase of enthalpy difference between inlet and outlet of evaporator. On the other hand, on the injection mode, cooling capacity increases sharply with the increase of injection ratio because mass flow rate in evaporator does not change nearly as shown in figure 11, but enthalpy difference in evaporator increases with an increase of subcooling degree. However, cooling capacity remains nearly constant from starting two-phase injection since subcooling degree and mass flow rate don't change. As shown in Figure 9, the subcooling degree at inlet of EEV is close to 0 °C when the bypass and injection ratio are 0.0 %. Therefore, subooling in the IHX is necessary for reliability of the system operation.

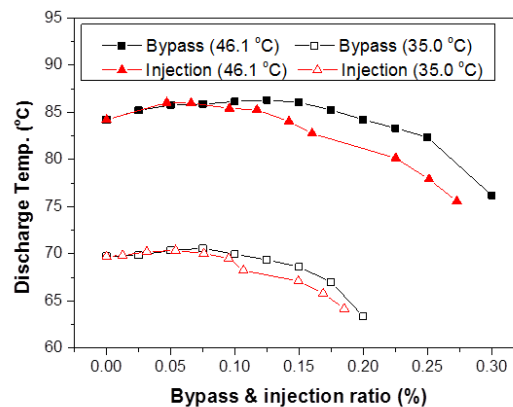


Figure 12 : Discharge temperature

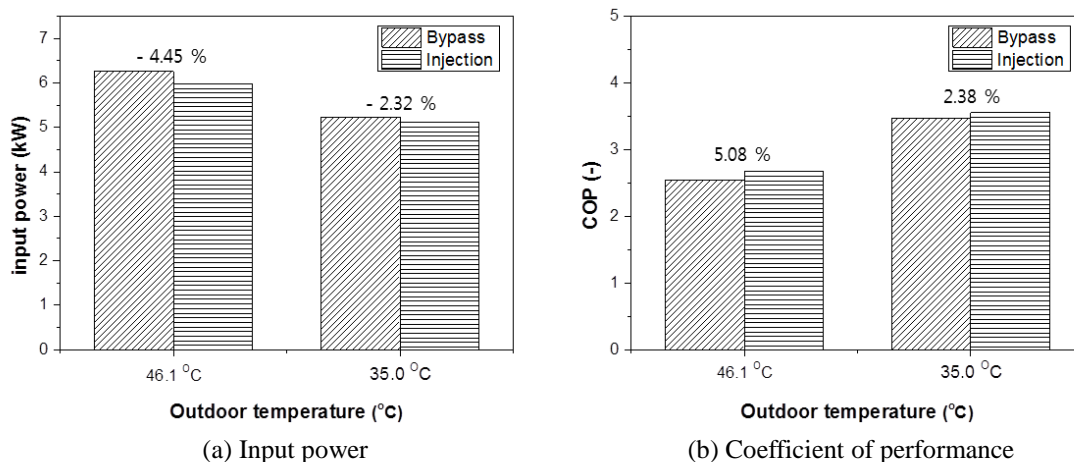


Figure 13 : Performance comparison of injection mode to that of bypass mode under same cooling capacity

Input power of two modes shows different trends as shown in Figure 7. On the bypass mode, input power doesn't change significantly with the increase of bypass ratio. On the injection mode, however, input power increases sharply due to the increase of total mass flow rate with injection mass flow rate as shown in Figure 11. Superheating degree at suction port for the bypass mode increases slightly with the increase of bypass ratio because the refrigerant from indoor units is mixed with bypass refrigerant of high superheating degree. However, superheating degree at suction port decreases with more increase of bypass ratio because of decrease of superheating degree at outlet of IHX. The low superheating degree at suction port improves compressor efficiency hence decreasing compressor input power as shown in Figure 7. On the injection mode, superheating degree is constant despite of variation in injection ratio. COP of the injection mode is lower than that of the bypass mode because of larger input power although cooling capacity on the injection mode is higher.

Figure 12 shows discharge temperature of a compressor with variation in bypass ratio and injection ratio. Discharge temperature increases slightly under small bypass and injection ratio, but it decreases with the increase of bypass and injection ratio. The reason for this phenomenon is different. On the bypass mode, discharge temperature decreases due to a decrease of suction temperature, but on the injection mode, it decreases with intercooling effect of refrigerant injection during compression process in a compressor.

Cooling capacity of the injection mode is higher than that of the bypass mode. Hence, input power and COP of the injection mode was compared to those of the bypass mode under maximum cooling capacity condition of the bypass mode. In order to operate the injection mode under the maximum cooling capacity of the bypass mode, compressor rotational speed was adjusted. Figure 13 (a) and (b) show comparison of input power and COP for two modes under same cooling capacity. As shown in Figure 13 (a), input power of the injection mode under two outdoor temperature conditions are reduced by 4.45 % and 2.32 %, respectively. Coefficient of performance of the injection mode was improved by 5.8 % and 2.38 %, respectively in Figure 13 (b). This is because the injection mode was operated with lower compressor rotational speed.

6. CONCLUSIONS

It is confirmed that the bypass and refrigerant injection cycle have potential to improve the performance of the multi-split VRF system and prevent flash gas generation in liquid pipeline. On the bypass mode, cooling capacity does not change significantly with variation in bypass ratio, but subcooling degree at inlet of EEV is enough to prevent flash gas generation. In addition, superheating degree at suction port of a compressor could be decreased by the bypass cycle because the bypass refrigerant in two-phase state is mixed with that heated from gas pipeline. On the refrigerant injection mode, cooling capacity and input power increase sharply with an increase of injection ratio due to increasing total mass flow rate with injection in a compressor. Discharge temperature of a compressor could be decreased by application of the bypass and injection cycle due to a decrease of suction temperature on the bypass mode, and an intercooling effect during compression process on the injection mode, respectively. When two modes are operated under same cooling capacity condition, input power of the multi-split VRF system with refrigerant injection is lower than that of the system with bypass cycle. This is because the refrigerant injection has potential to increase total mass flow rate in the system and enthalpy difference between inlet and outlet of evaporators.

NOMENCLATURE

A	flow area	(m^2)
C	flow coefficient	(-)
D	diameter	(m)
h	enthalpy	(kJ/kg)
k	specific heat ratio	(-)
L	length	(m)
m	mass	(kg)
R	ratio	(%)
V	Volume	(m^3)
v	specific volume	(m^3/kg)
W	work	(W)
θ	crank angle	(rad)

Subscript

in	inlet
out	outlet

inj	injection
u	upstream
ind	indicated
sub	subcooling
sh	superheating

REFERENCE

R. Afify, 2008, Designing VRF systems, ASHRAE Journal, Vol. 50, 52-55

Kwon et al., 2012, Field performance measurement of a VRF system with sub-cooler in educational building for the cooling season., Energy and Buildings, Vol. 49, 300-305

Li et al., 2016, Simulation on effects of subcooler on cooling performance of multi-split variable refrigerant flow systems with different lengths of refrigerant pipeline, Energy and Buildings, Vol. 126, 301-309

Cho et al., 2017, Performance comparison between R410A and R32 multi-heat pumps with a sub-cooler vapor injection in the heating and cooling modes, Energy, Vol. 112, 179-187

Kwon et al., 2017, Performance evaluation of a vapor injection heat pump system for electric vehicles, International Journal of Refrigeration, Vol. 74, 138-150

Chen et al. 2002, Mathematical modeling of scroll compressors-part I: compression process modeling., International Journal of Refrigeration, Vol. 25, 731-750

JSRA, 2018, Compressors for Air Conditioning and refrigeration, Japan society of Refrigeration and Air Conditioning Engineers.

Ragazzi F. and Pedersen C. O., 1995, Thermodynamic Optimization of Evaporators with Zeotropic Refrigerant Mixtures, ACRC TR-74, 47-54

Churchill, S.W., 1977, Friction-factor equation spans all fluid-flow regimes, Chemical Engineering Vol. 84(24), 91-92

ACKNOWLEDGEMENT

This work was supported by “Human Resources Program in Energy Technology” of the Korea Institute of Energy Technology Evaluation and Planning (KETEP), granted financial resource from the Ministry of Trade, Industry & Energy, Republic of Korea. (No. 20164010201000)